

# Status and Performance of the CDF Run II Silicon Detector

Tuula Maki  
on behalf of the CDF Collaboration

*University of Helsinki and Helsinki Institute of Physics,  
Fermilab - M.S. 318, P.O.Box 500, Batavia, IL 60510, USA*

---

## Abstract

The CDF silicon detector is one of the largest silicon detectors in operation. It has a total of 722,432 electronic channels, and it covers a sensor surface area of 6 m<sup>2</sup>. The detector has been operating reliably for five years, and it has recorded 1.5 fb<sup>-1</sup> of data. This article discusses experiences of operating such a large, complex system as well as the longevity of the detector.

*Key words:* CDF, silicon detector

*PACS:* 81.05.Cy, 61.80.-x, 10.

---

## 1 Introduction

The Run II silicon detector allows CDF [1] to do precision tracking, and triggering on and identification of secondary vertices. The silicon system consists of three separate silicon micro-strip detectors which share a common infrastructure: SVX II, ISL and L00 (see Fig. 1).

The SVX II [2] is the core of the CDF silicon detector. It consists of five layers of double-sided silicon at radii between 2.5 and 10.6 cm, covering 90 cm along the beam direction. Each layer combines axial strips at  $\approx 60 \mu\text{m}$  pitch providing  $r\phi$  information on one side with either 1.2° small-angle stereo strips (at  $\approx 60 \mu\text{m}$  pitch) or 90° strips (at  $\approx 140 \mu\text{m}$  pitch) providing  $rz$  information. The twelve fold  $\phi$  symmetry of SVX II makes it possible to treat each 30° wedge as an independent tracker. The data from SVX II is used at the Level 2 Silicon Vertex Trigger (SVT) [3], which identifies displaced vertices coming from  $B$  fragmentation.

---

*Email address:* tmaki@fnal.gov, *Tel:* +1-630-840-8414 (Tuula Maki).

The Intermediate Silicon Layers (ISL) [4] were added to extend silicon tracking to large  $\eta$  and to link tracks between the outer wire chamber and SVX II. The ISL are composed of one central layer ( $|\eta| < 1.0$ ) and two outer layers ( $1.0 < |\eta| < 2.0$ ). Each double-sided ISL sensor features both axial strips and  $1.2^\circ$  stereo strips.

The L00 [5] is mounted directly on the CDF beam pipe at a radius of approximately 1.5 cm. The single-sided sensors are actively cooled and designed to withstand a high bias voltage to allow extended running long after type inversion of the sensors.

All three detectors use the custom designed SVX3D readout chip [6] which features deadtimeless operation with separate acquisition and readout cycles. The digitization logic includes on-chip common mode noise suppression and readout sparsification. Each wedge is controlled by a portcard mounted on the detector structure, which distributes low/high voltage and commands to the sensor modules and converts the outgoing chip data into an optical signal using DOIM (Dense Optical Interface Modules) [7] transceivers.

## 2 Commissioning

Several surprises were encountered during the commissioning of the CDF silicon detector, including blocked ISL cooling lines, failures of L00 power supplies, and noise pickup along long L00 analog readout cables. The most challenging of the commissioning problems were the wirebond resonances [8]. The wirebonds, perpendicular to the 1.4 T magnetic field, carry power for the SVX3D chips from the  $r\phi$  to the  $z$  side of the SVXII hybrids. Any current fluctuations would induce a Lorentz force on the wires. During consecutive, synchronous chip readouts this would drive the wires to resonance and cause them to break. A new VME board was introduced to prevent wirebond resonances. Since installation of the board, no further wirebond failures have been found.

## 3 Operational experience and detector performance

Accessing the silicon sensors is impossible and therefore maintaining the high level of performance for the next three years is a significant challenge. Daily operations require about 5 FTEs from post-docs and graduate students. There are always two Silicon Operations Group members on call to ensure detector performance and safety.

Due to the proximity of the CDF silicon detector to the Tevatron beam line, it is particularly sensitive to any abnormal or unstable beam conditions. The

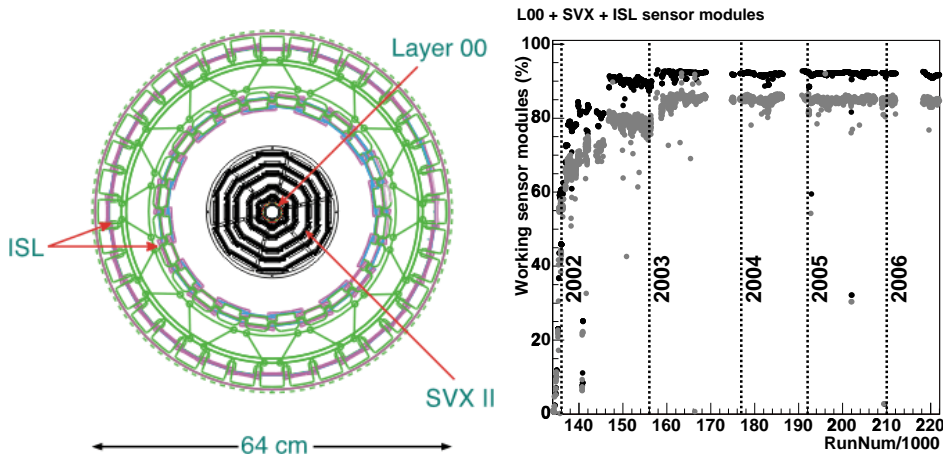


Fig. 1. Left:  $r\phi$  view of the silicon detector. Right: Percentage of working sensor modules over time. Powered sensor modules are shown in black, grey dots denote the sensor modules which are delivering data with digital error rates of less than 1%.

beam incidents can generate a shower of medium energy secondary particles hitting the silicon detector. The front-end chips have been most affected during beam incidents. We presume the reason for these failures is because the large instantaneous charge dose induces large currents, which may cause the permanent loss of communication with the affected chip. Due to the daisy-chain design, all the chips downstream on the sensor module are also lost. However, it has been observed that a large number of these affected chips have recovered after a period of inactivity.

Silicon tracking makes precision vertexing possible, which in turn makes possible identification of primary and secondary vertices in events with heavy flavour quark jets. The stable operation and efficient performance of the CDF silicon detector have had a significant contribution to recent  $B_s$  mixing results [9] as well as top quark mass measurements in  $b$ -tagged events [10].

Approximately 84% of SVX II, 82% of ISL and 96% of L00 produce data with a digital error rate smaller than 1%. These numbers have stayed constant since the mitigation of the wirebond resonance problem, see Fig. 1.

#### 4 Radiation damage and lifetime studies

The silicon detector lifetime will be limited by radiation damage. The main limiting factors are the inability to deplete the sensors or the decreased S/N ratio which seriously reduces the efficiency of the SVT and  $b$ -tagging.

Sufficient charge collection efficiency is achieved by applying a bias voltage between the two sides of each silicon sensor. Under irradiation and annealing,

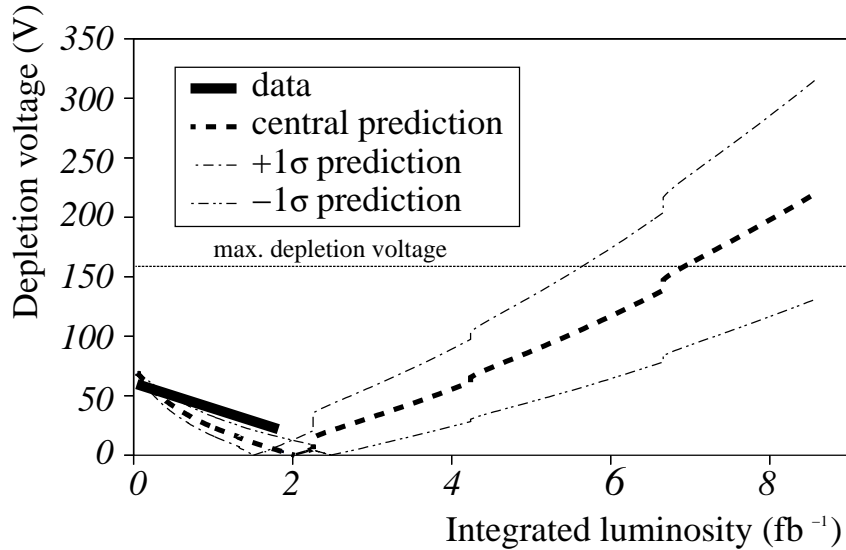


Fig. 2. Predictions of the voltage required for bulk depletion in SVX L0 together with depletion voltage measurements from data.

the required voltage evolves as the sensor bulk gradually changes from net  $n$ -type to  $p$ -type. After type inversion, the required voltage to fully deplete the silicon sensors increases. In SVX II, the capacitively coupled readout design limit the maximum bias voltage which can be applied.

We can measure the depletion voltage with two methods. The first one requires that beam is available. Then the bias voltage is varied and the change in collected charge is recorded. The bias voltage at which the collected charge has saturated is defined as the depletion voltage. The second method is to vary the bias voltage and measure the change in noise. The depletion voltage is defined as the bias which minimizes the noise. Predictions of the voltage required for bulk depletion in SVX L0 [11] together with depletion voltage measurements [12] are shown in Fig. 2. The measurements follow the optimistic prediction, which suggests that a failure to deplete the sensors is not a concern.

We have measured signal-to-noise ratio (S/N) from  $J/\psi$  dimuon events. We define the path length corrected cluster charge as “signal” and the average strip noise in the cluster as “noise”. After  $1.7 \text{ fb}^{-1}$  of delivered luminosity, the measured S/N on SVX II layers is between 9.5 and 12. S/N values are similar on both sides of sensors.

SVT sets a benchmark for S/N: the trigger efficiency is expected to start decreasing at  $\text{S/N} < 8$ . An empirical model was used to fit the data and predict the S/N as a function of integrated luminosity. In this model, the signal is expected to decrease linearly with integrated luminosity, and the noise is expected to increase as the square-root of the integrated luminosity. Figure 3 shows S/N predictions together with the measurements. According to these

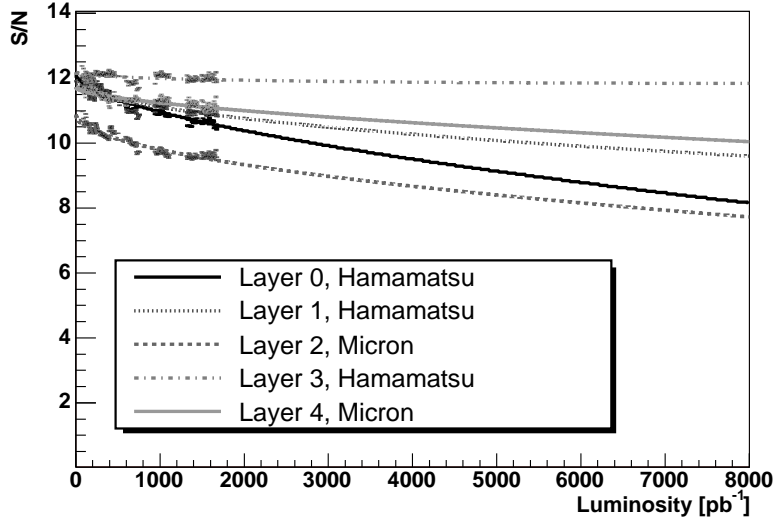


Fig. 3. Measured signal-to-noise ratios together with predictions for SVX II layers. The sensors for layers 0, 1, 3 are manufactured by Hamamatsu, 2, 4 by Micron.

predictions, S/N will not constrain detector performance in Run II.

Several actions have been taken to ensure the longevity of the CDF silicon system. The operating temperature of SVX II has been reduced from  $-6^{\circ}\text{C}$  to  $-10^{\circ}\text{C}$ , and the detector volume was thermally isolated. Operating the detector at a lower temperature and minimizing the number of thermo-cycles reduces the effects of radiation damage.

## References

- [1] D. Acosta et al., Phys. Rev. D 71 (2005) 032001
- [2] A. Sill et al., Nucl. Instrum. Meth. A447 (2000) 1-8.
- [3] W. Ashmanskas et al., Nucl. Instrum. Meth. A518 (2004) 532.
- [4] A. Affolder et al., Nucl. Instrum. Meth. A453 (2000) 84-88.
- [5] C. S. Hill et al., Nucl. Instrum. Meth. A511 (2003) 118-120.
- [6] M. Garcia-Sciveres et al., Nucl. Instrum. Meth. A435 (1999) 58-64.
- [7] S. Hou et al., Nucl. Instrum. Meth. A511, (2003) 166.
- [8] G. Bolla et al., Nucl. Instrum. Meth. A518 (2004) 277-280.
- [9] A. Abulencia et al., submitted to Phys. Rev. Lett., hep-ex/0609040
- [10] A. Abulencia et al., Phys. Rev. Lett. 96, 022004 (2006).
- [11] S. Worm et al., Nucl. Instrum. Meth. A549 (2005) 126-129.
- [12] A. Boveia et al., PoS HEP2005 (2005) 377.